

Published in final edited form as:

*J Micromech Microeng.* 2013 October ; 23(10): . doi:10.1088/0960-1317/23/10/107002.

## Scalable synthesis of a biocompatible, transparent and superparamagnetic photoresist for microdevice fabrication

P K Shah<sup>1</sup>, M R Hughes<sup>2</sup>, Y Wang<sup>2</sup>, C E Sims<sup>2</sup>, and N L Allbritton<sup>1,2</sup>

<sup>1</sup>Department of Biomedical Engineering, University of North Carolina, Chapel Hill, NC 27599, USA and North Carolina State University, Raleigh, NC 27695, USA

<sup>2</sup>Department of Chemistry, University of North Carolina, Chapel Hill, NC 27599, USA

### Abstract

The functionalization of photoresists with colloids has enabled the development of novel active and passive components for microfabricated devices. Incorporation of colloidal particles often results in undesirable reductions in photolithographic fidelity and device transparency. We present a novel photoresist composite incorporating poly(methyl methacrylate-co-methacrylic acid) (PMMA/MMA), the epoxy resin 1002F and colloidal maghemite nanoparticles to produce a stable, transparent and biocompatible photoresist. The composite photoresist was prepared in a scalable fashion in batches up to 1 kg with the particles remaining dispersed during room-temperature storage for at least 6 months. Following photolithography to form films, the nanoparticle size remained well below that of visible-light wavelengths as demonstrated by electron microscopy. Structures fabricated from the photoresist by conventional photolithography displayed aspect ratios greater than ten. When grown on the photoresist, the metabolic rate of HeLa cells was unchanged relative to cells grown on glass. Primary murine mesenchymal stem cells also displayed a normal morphology on the resist surface. The ability to manipulate microstructures formed from the composite was demonstrated by magnetically collecting clonal colonies of HeLa cells from a micropallet array. The transparency, biocompatibility, scalable synthesis and superparamagnetic properties of the novel composite address key limitations of existing magnetic composites.

### 1. Introduction

The generation of nanocomposite photoresists with modified properties has dramatically expanded the toolbox available for the integration of active and passive components into microdevices. Nanocomposites have been developed to confer properties of ferro- and superparamagnetism for mechanically actuatable devices[1-5], conductivity for the integration of electrodes[6-9], high dielectric constants for integrated capacitors[10], low internal stress for improving mechanical properties[11] and a low index of refraction for the generation of on-chip optical waveguides[12]. These composites have typically relied upon the addition of insoluble components, often nanoparticles, into the photoresist. A common feature among nanocomposites incorporating metallic colloids is reduced accuracy in reproducing mask features, diminished fabrication quality and poor optical clarity. This undesirable optical property is generally due to an uneven distribution of the colloid in the photoresist as a result of aggregation. For biological applications where optical clarity is critical for analysis and imaging, transparent nanocomposite photoresists would prove valuable. Gach et al[1] demonstrated a method for dispersing iron oxide nanoparticles in photoresist that yielded high-fidelity, optically clear structures. This method, however, required high-intensity ultrasonication to prevent nanoparticle aggregation and was not amenable to production in large batches. In addition, the resulting photoresist was limited to

aspect ratios of 4:1, offering no improvement in mechanical properties over the native 1002F photoresist it was based upon.[13]

To address these issues, we present a novel photoresist composite incorporating the epoxide-based photoresist 1002F and poly(methyl methacrylate-co-methacrylic acid) (PMMA/MMA). To test the photolithographic performance of the PMMA/1002F-based photoresist, arrays of microposts of varying diameters were fabricated and imaged by scanning electron microscopy (SEM). The dispersion of the maghemite nanoparticles in the PMMA/1002F composite was evaluated by imaging 100 nm-thick sections of the cross-linked composite by transmission electron microscopy (TEM). The spectral transmittance of the 0.25% (w/w) maghemite PMMA/1002F composite was measured by UV-Vis spectroscopy and the reaction of PMMA/MMA with the 1002F epoxy was confirmed by differential scanning calorimetry (DSC). The effect of the maghemite PMMA/1002F composite surface on cellular metabolism was tested by tracking the metabolic activity of HeLa cells over 72 h. Additionally, the compatibility of the composite surface with primary cell culture was evaluated by culturing murine mesenchymal stem cells for 72 h and observing cell morphology. The functionality of the magnetic composite was assessed by isolating single adherent cells cultured on an array of individually removable magnetic cell carriers.[14,15]

## 2. Methods

### 2.1 Synthesis of maghemite nanoparticles

A solution of 10-nm maghemite nanoparticles in toluene was prepared using the method described by Gach et al.[1] Iron salts (23.82 g FeCl<sub>2</sub> and 38.94 g FeCl<sub>3</sub> in 3 L of deionized (DI) water) were precipitated by the addition of a strong base (240 mL of 14.5 M NH<sub>4</sub>OH), and washed three times with DI water by magnetic decantation. After resuspension in 480 mL of 1.5 M HNO<sub>3</sub>, 104 g of Fe(NO<sub>3</sub>)<sub>2</sub> was added to the solution which was then heated to boiling for 1 h. After cooling to 25 °C the precipitate was again washed by magnetic decantation once with 480 mL of 1.5 M HNO<sub>3</sub>, once with 2500 mL of 0.1 M NH<sub>4</sub>OH and resuspended in 1500 mL of DI water. 90 g of oleic acid was added to the suspension and mixed for 15 minutes. The excess oleic acid and water were removed from the precipitate by three successive extractions with 200 mL of 100% ethanol. The precipitate was then dissolved in 800 mL of toluene and stored in amber glass bottles until use.

### 2.2 Composite preparation

Maghemite nanoparticles (3 g) were diluted with toluene (800 mL total volume). The weight percentage of maghemite nanoparticles in toluene was determined by evaporating solvent from a sample by heating at 120 °C for 30 min and weighing the dry solids. PMMA/MMA (100 g of methyl methacrylate:methacrylic acid at a molar ratio of 1:0.016, PMMA/MMA molecular weight =34,000, Sigma Aldrich, St. Louis, MO) was added to the nanoparticle solution and allowed to dissolve overnight while stirring. butyrolactone (233.3 g) was added drop-by-drop using a separatory funnel and stirred further for an additional 24 h. The toluene in the solution was then removed by roto-evaporation at 60 °C leaving a deep red, highly viscous polymer suspension. The superparamagnetic PMMA/MMA solution was then added directly to 1002F-50 photoresist (1:2.6 by mass, PMMA/MMA:1002F-50) which had been prepared as previously described.[13] The mixture was then placed on a bottle roller for 4 days. The resulting PMMA/1002F photoresist was deep red in color.

### 2.3 Characterization of PMMA/1002F photoresist and magnetic composite

Melting point and glass transition temperatures were determined by DSC with a Q200 calorimeter (TA Instruments, New Castle, DE). 1002F and PMMA/MMA samples were analyzed as pure powders packed into the DSC sample pans. The PMMA/1002F was

analyzed after 100  $\mu\text{L}$  of the polymer suspension was baked into the sample pan at 120  $^{\circ}\text{C}$  for 72 h under vacuum to completely remove the solvent. For optical characterization, 50  $\mu\text{m}$  thick films of 1002F photoresist, PMMA/1002F, and PMMA/1002F with 0.25% (w/w) maghemite nanoparticles were prepared by spin coating onto plasma-cleaned #2 glass coverslips. These films were treated as described below for micropallet fabrication before use except that no mask was used in producing UV-cross-linked films. Transmission spectra for triplicate preparations of each film were measured with a bare coverslip as a blank using a SpectraMax M5 spectrophotometer (Molecular Devices Corporation, Sunnyvale, CA). Working curves were generated by producing films of different thickness by varying the speed of the spin-coat step. The exposure needed to fully cross-link the films and form microstructures was then optimized and the final thickness of the film measured using a P-6 stylus profilometer (KLA Tencor, Milpitas, CA). The maximum aspect ratio of the PMMA/1002F with 0.25% maghemite nanoparticles composite was determined by fabricating a post-array using the protocol described below for fabrication of micropallet arrays. The fabricated structures were then imaged by SEM using a Quanta 200 environmental-SEM (FEI, Hillsboro, OR). The dispersion of maghemite nanoparticles into the PMMA/1002F photoresist was characterized by imaging transverse slices of a 50- $\mu\text{m}$  thick film of the magnetic PMMA/1002F composite photoresist by TEM (JEOL 100CX II). The film was set in Polybed 812 resin and cured at 65  $^{\circ}\text{C}$  overnight. 100 nm thick sections of the film were cut with an ultramicrotome prior to imaging.

#### 2.4 Cell culture and proliferation assay

Uniform films of PMMA/MMA, 1002F-50 and PMMA/1002F with 0.25% (w/w) maghemite nanoparticles as well as bare glass slides were treated with an air plasma (Harrick Plasma, Ithaca, NY) for 5 min after being affixed to 4-well arrays fabricated from polylactic acid (PLA) with a benchtop 3D-printer (BFB-3000, Bits from Bytes Inc., Clevedon, UK). Polydimethylsiloxane (PDMS) was used to glue the wells to the surfaces. HeLa cells were plated in 3 of 4 wells of each array at a density of 2000 cells per well in 100  $\mu\text{L}$  of culture media and cultured for 24, 48 or 72 h. Medium in each well was replaced every 24 h. A standard cell proliferation assay (MTT) was performed at multiple time points in accordance with the manufacturer's instructions (Life Technologies, Grand Island, NY). Briefly, 10  $\mu\text{L}$  of 5 mg/mL (3-(4,5-dimethylthiazol-2-yl)-2,5-diphenyltetrazolium bromide (MTT) was added to each of 3 sample wells and one control well containing no cells and incubated at 37  $^{\circ}\text{C}$  for 4 h. MTT is metabolized by cells into an insoluble purple formazan which is then solubilized by the addition of 100  $\mu\text{L}$  of 100 mg/mL sodium dodecyl sulfate (SDS) in 0.01 M HCl followed by incubation at 37  $^{\circ}\text{C}$  for 4 h. 100  $\mu\text{L}$  of fluid from each well was sampled and absorbance measurements were taken at 570 nm using a spectrophotometer. To test the compatibility of the composite with primary cell growth, mesenchymal stem cells (MSC) were derived from the long bone of a mouse [13] and plated on conventional tissue-culture dishes or films of the magnetic PMMA/1002F composite in Dulbecco's Modified Eagle Medium (DMEM) with 10% fetal bovine serum and cultured for 72 h.

#### 2.5 Single-cell isolation by magnetic micropallet release

Micropallet arrays were fabricated according to previously reported protocols.[14-17] A 70  $\mu\text{m}$  thick film of PMMA/1002F 0.25% (w/w) maghemite nanoparticles was spin coated onto 75 $\times$ 25 mm glass slides. The solvent was evaporated from the film by baking in a 95  $^{\circ}\text{C}$  oven for 60 min. The PMMA/1002F with 0.25% (w/w) maghemite nanoparticles required 7 $\times$  higher exposure energies to fully cross-link the polymer as compared to similar features fabricated in native 1002F-50. Fabricated arrays were then treated with air plasma for 5 min prior to coating the arrays by low-pressure vapor deposition of (heptadecafluoro-1, 1, 2, 2-tetrahydrodecyl)trichlorosilane as previously described.[17]

The micropallet array was then glued with PDMS onto a cassette fabricated from acrylonitrile butadiene styrene (ABS) by means of a 3-D printer. The PDMS was cured in a 70 °C oven for 30 min. Prior to use, the array was sterilized by rinsing with 70% ethanol and air-drying under a germicidal UV lamp for 30 min. The surface of the micropallet array was coated with fibronectin by incubating the array in 1 mL of 25 µg/mL fibronectin in phosphate-buffered saline (PBS) for 30 min at 25 °C. The array was then rinsed 3 times with PBS and finally immersed in Dulbecco's Modified Eagle Medium (DMEM) with 10% fetal bovine serum. A suspension of HeLa cells expressing GFP (10,000 cells in 3 mL) was added to each cassette and the cells were allowed to settle and adhere to the pallets overnight. The cells were imaged the following day, and cultured on the micropallet array for 2 additional days to allow clonal colonies to form. Prior to release, the micropallet cassette was mated to the bottom of a 47 mm diameter Petri dish (BD Biosciences, San Jose, CA) which had been treated with air plasma for 10 min and sterilized using the protocol described above. The magnetic collection experiment was carried out as described by Gach et al.[1] The clonal colonies were released by focusing a 5 ns pulse from an Nd:YAG laser at the photoresist-glass interface through a 20×, 0.7 N.A. objective and collected against gravity by a ring-shaped rare earth magnet (K&J Magnetics) placed on the collection plate. The cassette was designed to reduce the gap between the array and the collection plate to 3 mm. After collection, the Petri dish was removed from the cassette with the magnet, inverted and filled with an expansion media consisting of 50% FBS, 25% HeLa-GFP conditioned DMEM and 25% fresh DMEM. The conditioned media was generated by incubating 20 mL of fresh DMEM on a culture of HeLa cells on a 75 mm<sup>2</sup> tissue culture flask at 50% confluency for 24 hours. The conditioned media was then aspirated and filtered through a 0.22 µm nylon filter and stored at 4 °C for less than 72 h before use. The released clonal colonies were imaged again after 3 days to confirm their viability and to observe the expansion of the colony onto the Petri dish surface.

### 3. Results

#### 3.1 Characterization of PMMA/1002F photoresists

Previous protocols to stably disperse maghemite nanoparticles into pure 1002F photoresist proved difficult to scale. Polymer additives were explored for their potential to stabilize the maghemite nanoparticles while forming a single phase with the photoresist. PMMA/MMA was selected as an additive to the 1002F photoresist system for its optical clarity, high glass transition temperature and the presence of acidic groups which could react with epoxides in the 1002F as well as stabilize the nanoparticles. The glass transition of PMMA/MMA occurred at 110 °C (figure 1A). Un-crosslinked 1002F was observed to melt at 56.8 °C. When a mixture of PMMA/MMA and 1002F was heated from 40 °C to 140 °C, the material did not melt and a single glass transition was observed at 110 °C, supporting the conclusion that covalent bonds were formed between the 1002F and PMMA/MMA to form a single phase.

In order to maintain optical clarity for imaging and photolithographic fidelity, maghemite nanoparticles <20 nm in diameter were used to generate a magnetic photoresist. Oleic acid-capped nanoparticles rapidly aggregated when mixed directly into the GBL-based solutions of PMMA/MMA or 1002F and cured (figure 1.C). To prevent particle aggregation during solvent mixing, the PMMA/MMA was initially dissolved in toluene followed by addition of nanoparticles in the same solvent. GBL was then slowly introduced into this toluene-based solution. The magnetic nanoparticles remained dispersed in the solvent mixture and after evaporation of the toluene leaving the PMMA/MMA and nanoparticles dissolved in GBL alone. The PMMA/MMA/nanoparticle solution was then mixed into a solution of 1002F with GBL as the solvent. The nanoparticles showed no visible aggregation or phase separation after the composite photoresist was cured when examined by light microscopy

(figure 1.D). When viewed by electron microscopy, the cross-linked magnetic PMMA/1002F composite possessed nanoparticle aggregates of 200 nm or less (figure 1.E). When examined by spectrophotometry, the cross-linked photoresist remained transparent at visible wavelengths greater than 500 nm (figure 1.B). The marked absorbance increase in the UV wavelengths resulted in a 4-fold increase in the exposure dose required for photolithography of the nonmagnetic PMMA/1002F photoresist and a 7-fold increase relative to that of 1002F photoresist. The 0.25% (w/w) maghemite PMMA/1002F composite showed no signs of visible aggregation or flocculation after more than 6 months of storage at room temperature in an amber glass bottle. The magnetic PMMA/1002F composite was produced in batches as large as 1 kg.

### 3.2 Photolithographic performance of PMMA/1002F photoresists

Previous reports of 1002F-based photoresists demonstrated an aspect ratio of 4:1.[14] Higher aspect ratios up to 20:1 have been demonstrated for SU-8, a related photoresist.[18] The maximum aspect ratio achievable by conventional UV photolithography with the PMMA/1002F photoresist was evaluated by preparing films of varying thickness and optimizing the total UV exposure energy through a test pattern containing circular holes ranging from 1 to 10  $\mu\text{m}$  in diameter (figure 2). When circular posts were fabricated, the PMMA/1002F composite with 0.25% (w/w) maghemite nanoparticles provided aspect ratios exceeding 10:1 (figure 2.C). The smallest feature successfully produced in these photoresists was 4  $\mu\text{m}$ , the smallest diameter tested. The features shown (figure 2.C and D) were fabricated 3 months after the initial preparation of the maghemite PMMA/1002F composite demonstrating the long-term stability of the photoresist.

### 3.3 Cell culture on PMMA/1002F photoresist surfaces

Biocompatibility is an important consideration in selecting materials for fabricating microdevices for biological applications.[19,20] Data in the literature suggests that iron oxide nanoparticles can be cytotoxic.[21,22] A series of metabolic assays using MTT were performed over a 72-h period to assess the effects of the magnetic PMMA/1002F composite and its various components on cell growth and metabolism. Three substrates were prepared from each of the following, PMMA/MMA, PMMA/1002F, PMMA/1002F with 0.25% (w/w) maghemite particles, 1002F, and untreated glass. An MTT assay was performed on HeLa cells cultured on the substrates at 24, 48 and 72 h after seeding (figure 3.A). The PMMA/1002F with nanoparticles showed no statistically significant ( $p = 0.05$ ) effect on the growth and metabolism of these cells relative to a glass surface. Additionally, mesenchymal stem cells (MSC) derived from murine long bone grown on films of the magnetic PMMA/1002F composite displayed typical morphologies compared with that exhibited by cells grown in conventional tissue-culture dishes (figure 3.B).

### 3.4 Single-cell isolation using magnetic micropallet arrays

Recent improvements in the sensitivity of molecular assays and growing recognition of the importance of heterogeneity in biological systems have highlighted the need for parallel improvements in single-cell isolation platforms.[23] Micropallet arrays have been demonstrated as an efficient platform for performing single-cell isolation from samples of varying size and diversity.[15-17] The use of a transparent, magnetic photoresist in the fabrication of micropallet arrays enables the facile collection of cells, preventing contamination with undesired cells and allowing multiplexed isolation by collecting released micropallets into microwell arrays.[1]

A cassette for single-cell isolation was developed by mating micropallet arrays fabricated superparamagnetic PMMA/1002F with polystyrene Petri dishes (figure 4.A). The upper lid of the Petri dish was used as a pallet-collection plate (figure 4.A). HeLa cells stably



expressing a histone-H2B-GFP fusion protein were seeded onto an array of superparamagnetic micropallets (200 elements  $\times$  200 elements) coated with fibronectin, incubated at 37 °C overnight, and imaged (figure 4.B). After 2 d in culture, the individual cells expanded into clonal colonies on each micropallet (figure 4.C). After laser-based release, Selected micropallets with cells were released by a laser (n=5) and then collected onto the Petri dish lid by application of a magnetic force. The isolated colonies were followed over time and 100% of the colonies continued to proliferate with increased cell numbers (figure 4.D).

## 4. Conclusions

A highly scalable process for producing transparent, magnetic photoresist was developed enabling kilogram-sized batches to be synthesized. The resulting magnetic composite photoresist was capable of forming microstructures with aspect ratios greater than 10. Microstructures formed from the magnetic composite photoresist were highly transparent in the visible spectrum, were compatible with conventional fluorescence imaging and mammalian cell culture (including primary cell culture) and were used to fabricate magnetically active structures with demonstrated applications in single-cell isolation. The excellent optical and biological properties of the magnetic composite photoresist demonstrate its potential value for a wide variety of applications such as cell manipulation, the production of magnetic meta-materials, and fabrication of magnetically actuatable microsystems.

## Acknowledgments

This research was supported by grants from the National Institutes of Health (EB012549 and HG004843). The authors would like to thank Wallace Ambrose for his assistance with TEM imaging and Sarah M. Brosnan for her assistance in generating the DSC data.

## References

1. Gach PC, Sims CE, Allbritton NL. Transparent magnetic photoresists for bioanalytical applications. *Biomaterials*. 2010; 31:8810–7. [PubMed: 20719380]
2. Damean N, Parviz BA, Lee JN, Odom T, Whitesides GM. Composite ferromagnetic photoresist for the fabrication of microelectromechanical systems. *J Micromech Microeng*. 2005; 15:29–34.
3. Gunn NM, Chang R, Westerhof T, Li GP, Bachman M, Nelson EL. Ferromagnetic micropallets for magnetic capture of single adherent cells. *Langmuir*. 2010; 26:17703–11. [PubMed: 20968293]
4. Sakar MS, Steagar EB, Kim DH, Kim MJ, Pappas GJ. Single cell manipulation using ferromagnetic composite microtransporters. *Appl Phys Lett*. 2010; 96:043705.
5. Suter M, Graf S, Ergeneman O, Schmid S, Camenzind A, Nelson BJ, Hierold C. Superparamagnetic photosensitive polymer nanocomposite for micro and nanosystems. *IEEE Transducers*. 2009:869–872.
6. Benlarbi M, Blum LJ, Marquette CA. SU-8-carbon composite as conductive photoresist for biochip applications. *Biosens Bioelectron*. 2012; 38:220–5. [PubMed: 22705408]
7. Cong H, Pan T. Photopatternable Conductive PDMS materials for microfabrication. *Adv Funct Mater*. 2008; 18:1912–21.
8. Jiguet S, Bertsch A, Hofmann H, Renaud P. Conductive SU8 photoresist for microfabrication. *Adv Funct Mater*. 2005; 15:1511–16.
9. Li T, Hsu SL. Preparation and properties of conductive silver / photosensitive polyimide nanocomposites. *J Polym Sci A1*. 2009:1575–83.
10. Xu J, Wong CP. High dielectric constant SU8 composite photoresist for embedded capacitors. *J Appl Polym Sci*. 2006; 103:1523–8.
11. Jiguet S, Bertsch A, Judelewicz M, Hofmann H, Renaud P. SU-8 nanocomposite photoresist with low stress properties for microfabrication applications. *Microelectron Eng*. 2006; 83:1966–70.

12. Ruano-López JM, Aguirregabiria M, Tijero M, Arroyo MT, Elizalde J, Berganzo J, Aranburu I, Blanco FJ, Mayora K. A new SU-8 process to integrate buried waveguides and sealed microchannels for a lab-on-a-chip. *Sensor Actuat B-Chem.* 2006; 114:542–51.
13. Zhu H, Guo ZK, Jiang XX, Li H, Wang XY, Yao HY, Zhang Y, Mao N. A protocol for isolation and culture of mesenchymal stem cells from mouse compact bone. *Nat Protoc.* 2010; 5:550–60. [PubMed: 20203670]
14. Pai J, Wang Y, Salazar GT, Sims CE, Bachman M, Li GP, Allbritton NL. Photoresist with low fluorescence for bioanalytical applications. *Anal Chem.* 2007; 79:8774–80. [PubMed: 17949059]
15. Salazar GT, Wang Y, Young G, Bachman M, Sims CE, Li GP, Allbritton NL. Micropallet arrays for the separation of single, adherent cells. *Anal Chem.* 2007; 79:682–7. [PubMed: 17222037]
16. Wang Y, Young G, Bachman M, Li GP, Allbritton NL. Collection and expansion of single cells and colonies released from a micropallet array. *Anal Chem.* 2007; 79:2359–66. [PubMed: 17288466]
17. Wang Y, Sims CE, Bachman M, Li GP, Allbritton NL. Micropatterning of living cells on a heterogeneously wetted surface. *Langmuir.* 2006; 22:8257–62. [PubMed: 16952271]
18. Campo A, Greiner C. SU-8: a photoresist for high-aspect-ratio and 3D submicron lithography. *J Micromech Microeng.* 2007; 17:R81–95.
19. Walker GM, Zeringue HC, Beebe DJ. Microenvironment design considerations for cellular scale studies. *Lab Chip.* 2004; 4:91–7. [PubMed: 15052346]
20. Voskerician G, Shive MS, Shawgo RS, von Recum H, Anderson JM, Cima MJ, Langer R. Biocompatibility and biofouling of MEMS drug delivery devices. *Biomaterials.* 2003; 24:1959–67. [PubMed: 12615486]
21. Brunner TJ, Wick P, Manser P, Spohn P, Grass RN, Limbach LK, Bruinink A, Stark WJ. In vitro cytotoxicity of oxide nanoparticles: comparison to asbestos, silica, and the effect of particle solubility. *Envir Sci Tech.* 2006; 40:4374–81.
22. Pisanic TR, Blackwell JD, Shubayev VI, Fiñones RR, Jin S. Nanotoxicity of iron oxide nanoparticle internalization in growing neurons. *Biomaterials.* 2007; 28:2572–81. [PubMed: 17320946]
23. Almendro V, Marusyk A, Polyak K. Cellular heterogeneity and molecular evolution in cancer. *Annu Rev Pathol.* 2013; 8:277–302. [PubMed: 23092187]

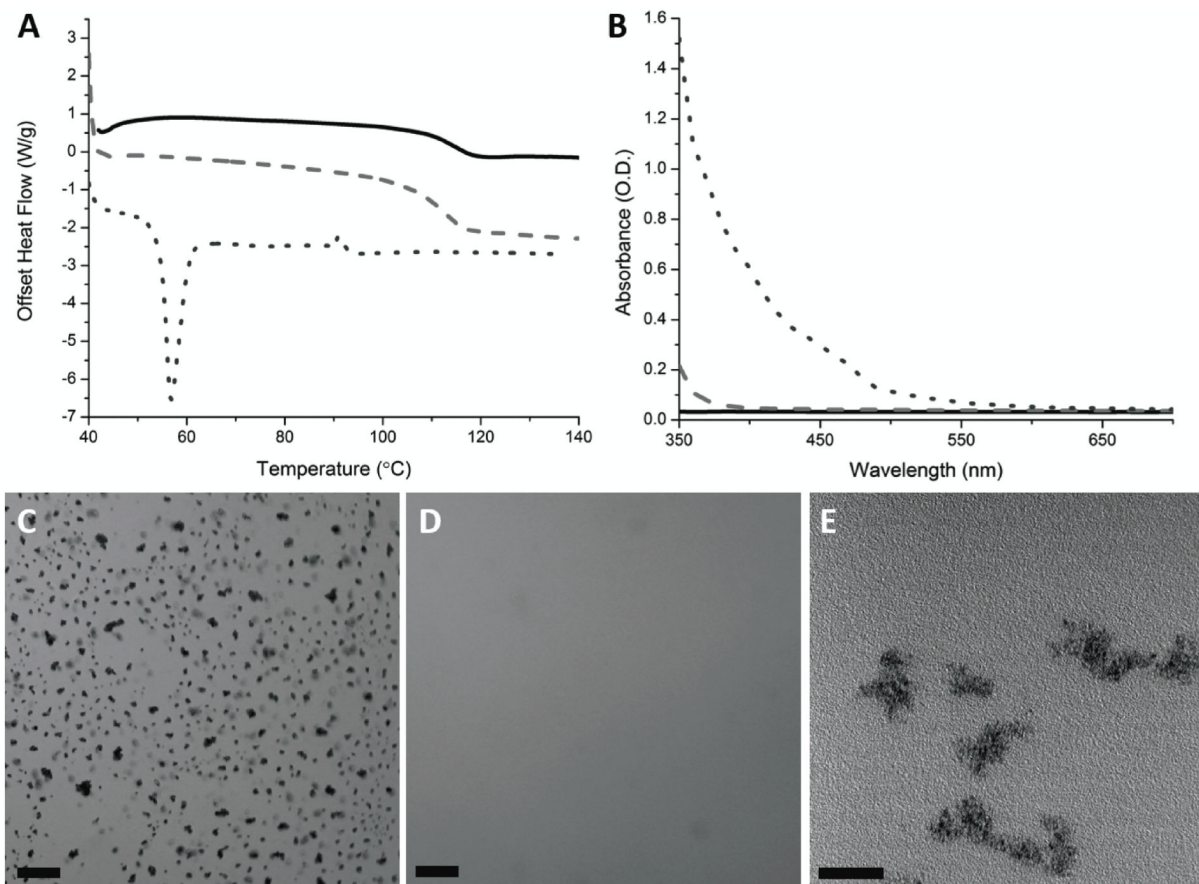


**Figure 1.**

(A) Heat flow curves of PMMA/MMA (dashed line), 1002F (dotted line) and PMMA/1002F (solid line) photoresist as measured by differential scanning calorimetry while heating at a rate of 10 °C/min. The curves for PMMA/MMA and PMMA/1002F photoresist have been offset by 3 and 4.5 W/g, respectively. (B) Absorbance spectra of 50- $\mu$ m thick films of PMMA/MMA (solid line), PMMA/1002F (dashed line) photoresist and PMMA/1002F with 0.25% (w/w) maghemite nanoparticles (dotted line). (C,D) Optical micrograph of a cured film produced from the direct addition of maghemite nanoparticles into 1002F photoresist (C) and of a film of PMMA/1002F with 0.25% (w/w) maghemite nanoparticles (D). The scale-bar is 50  $\mu$ m. (E) TEM of a transverse slice of a cured film of PMMA/1002F with 0.25% (w/w) maghemite nanoparticles. The scale-bar is 100 nm.



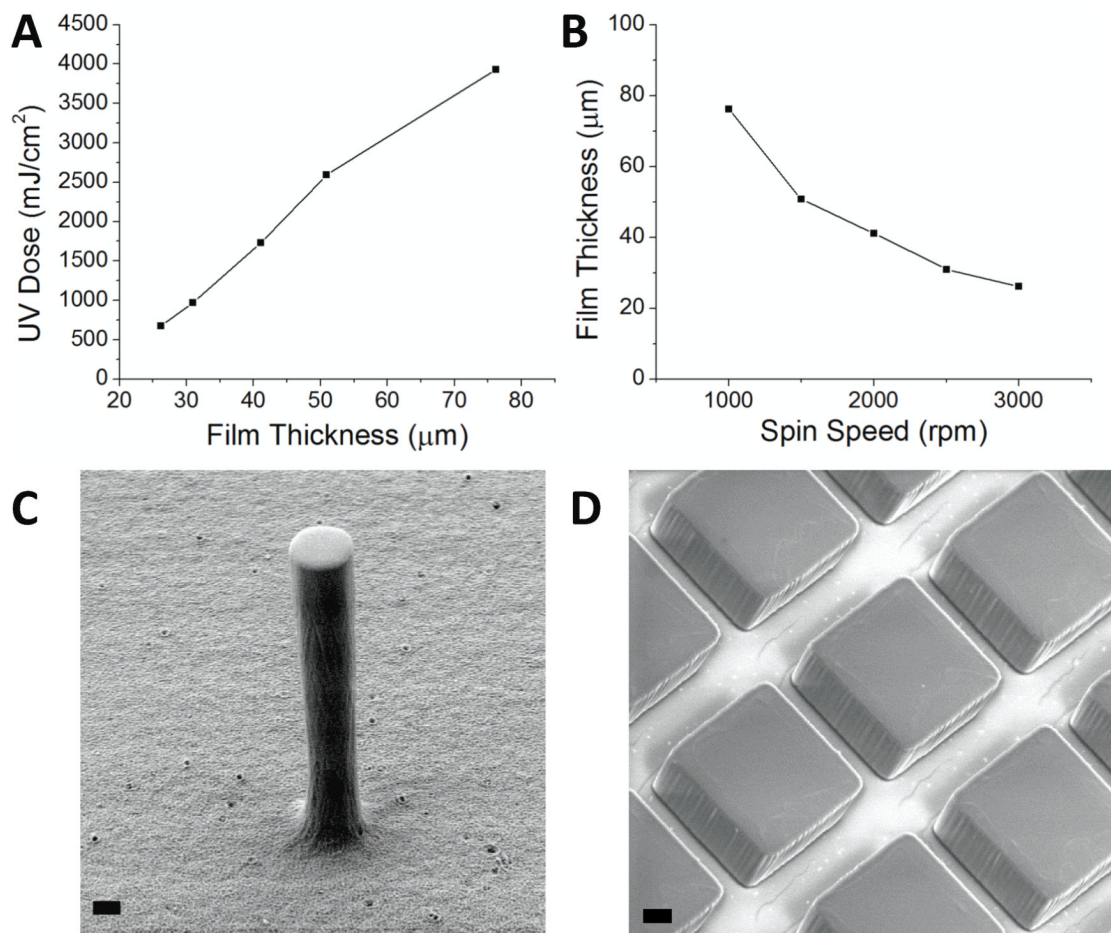


**Figure 2.**

SEM micrographs of microstructures fabricated from PMMA/1002F photoresists. (A) Working curve showing required UV dose to cross-link films of PMMA/1002F with 0.25% (w/w) maghemite nanoparticles of varying thicknesses ( $N=3$ , error bars not visible). (B) Relationship between spin speed and film thickness of PMMA/1002F with 0.25% (w/w) maghemite nanoparticles ( $N=3$ , error bars not visible). (C) Micropost ( $6 \times 72 \mu\text{m}$ , diameter  $\times$  height, aspect ratio = 12) fabricated from PMMA/1002F photoresist with 0.25% (w/w) maghemite nanoparticles. The scale-bar is  $6 \mu\text{m}$ . (D) Arrays of micropallets ( $100 \times 100 \times 50 \mu\text{m}$ ,  $L \times W \times H$ ). The scale-bar is  $10 \mu\text{m}$ .

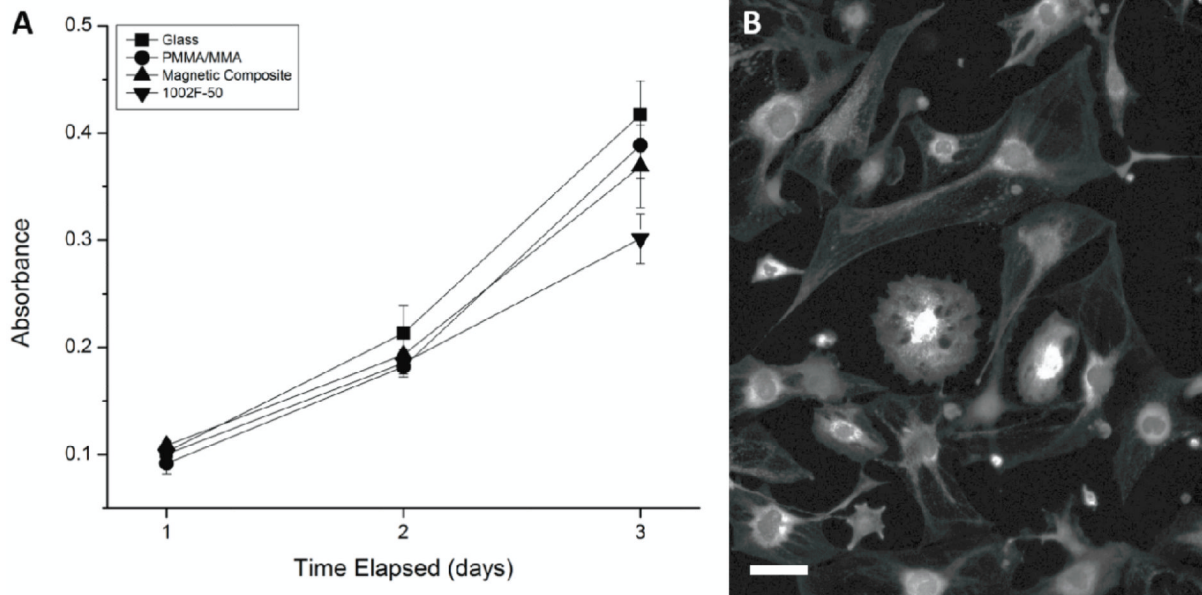


**Figure 3.** Biocompatibility of PMMA-containing photoresists. (A) Measurement of MTT metabolism by HeLa cells cultured on test substrates over 72 h. (B) Murine MSCs cultured on a film of PMMA/1002F with 0.25% (w/w) maghemite nanoparticles. The scale-bar is 100  $\mu\text{m}$ .

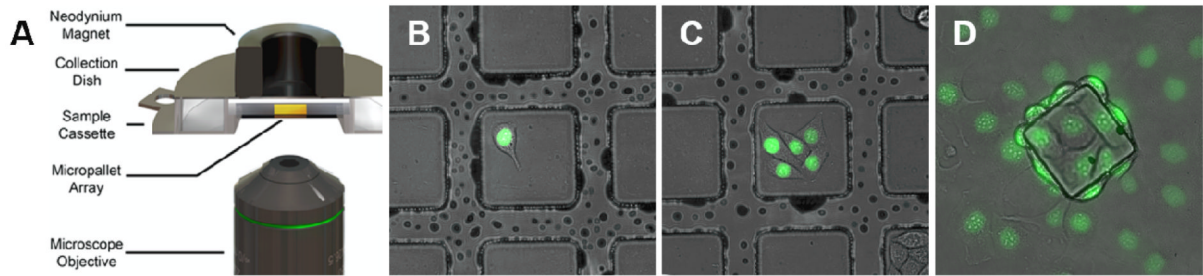


**Figure 4.**

(A) Schematic of experimental setup for single-cell isolation. Cells were loaded onto a micropallet array (each micropallet is  $100 \times 100 \times 50 \mu\text{m}$  L $\times$ W $\times$ H) mounted in a cassette. A laser pulse focused at the photoresist-glass interface through a 0.7 N.A. objective was used to release individual micropallets from the array which were then attracted upward to the collection dish by the neodymium magnet. (B) A single HeLa cell possessing a fluorescent nucleus indicating expression of the histone-H2B-GFP fusion protein growing for 24 h on a micropallet array fabricated from the magnetic PMMA/1002F composite. (C) After 48 h in culture, the single cell expanded into a colony. (D) The micropallet in “C” shown 96 h after release and collection demonstrating that the colony continued to expand with cells migrating from the micropallet onto the collection well surface. Panels B-D are overlaid brightfield and fluorescence images.